Applied Thermal Engineering 29 (2009) 2999–3005

Contents lists available at ScienceDirect

Applied Thermal Engineering

journal homepage: www.elsevier.com/locate/apthermeng

System dynamics model and startup behavior of loop heat pipe

B.J. Huang *, H.H. Huang, T.L. Liang

Department of Mechanical Engineering, National Taiwan University, Taipei, Taiwan

ARTICLE INFO

Article history:
Received 28 February 2008
Accepted 21 March 2009
Available online 28 March 2009

Keywords:
Loop heat pipes
Startup of loop heat pipe
Transient performance of a LHP

ABSTRACT

The purpose of this article is to study the system dynamics model and startup behavior of loop heat pipe. A mathematical model in normal operation was derived from the experimental data. The model is presented as a matrix of second-order transfer functions. It is found that the system dynamics of a LHP is a variable-structure system that changes with operating conditions. The startup phenomena are studied experimentally. The startup phenomena of a LHP can be classified into four modes, based on the heat load: (1) failure mode: $\dot{Q}_{in} < \dot{Q}_{min}$, (2) oscillating mode: $\dot{Q}_{min} < \dot{Q}_{in} < \dot{Q}_{crit}$, (3) overshoot mode: $\dot{Q}_{crit} < \dot{Q}_{in} < \dot{Q}_s$, and (4) normal mode: $\dot{Q}_s < \dot{Q}_{in}$. For heat load $\dot{Q}_{in} < 40\,\mathrm{W}(\dot{Q}_s)$, the overshoot phenomenon is observed. For $20\,\mathrm{W}(\dot{Q}_{crit}) < \dot{Q}_{in} < 40\,\mathrm{W}(\dot{Q}_s)$, the oscillation phenomenon is observed. For $\dot{Q}_{in} < 5\,\mathrm{W}(\dot{Q}_{min})$, the startup failure is observed. All the startup behavior is of second- order.

1. Introduction

A loop heat pipe (LHP) is a passive heat-transfer device that uses micro-scale wick technology which can transfer a large amount of heat over a long distance through a flexible pipe and has a good anti-gravity performance [1].

Fig. 1 shows the schematic of a LHP. A LHP consists of an evaporator, a condenser, a compensation chamber, and liquid and vapor lines. The evaporator is made of a wick (capillary material) that is inserted in a case and has a liquid channel in the core. The liquid line directly connects to the compensation chamber and transfers working fluid to the liquid channel of the wick. Heat is absorbed at the outer surface of the evaporator. There are several vapor channels (grooves) at the outer surface of the wick which admit vapor flowing out of the evaporator and into the vapor line [2].

There is a startup condition for the LHP which requires a temperature difference across the wick structure according to the following equation [3]:

$$\Delta P_{tot} - \Delta P_w = (\mathrm{d}P/\mathrm{d}T)(T_e - T_{cc}) \tag{1}$$

The relationship of Eq. (1) is important for minimal startup heat load and temperature overshoot. The startup of a LHP is a behaviour of dynamic system that is very complex. The factors affecting the startup of a LHP include the design of compensation chamber and evaporator, the initial state of working fluid in the evaporator, the charge volume of working fluid, the attitude of LHP and the initial state of a LHP before heat loads are applied. Two phenomena were observed very often in the startup of a LHP: (1) temperature overshoot and (2) minimal heat load to startup [4].

The understanding of system dynamics behaviour of a LHP is important for predicting its performance during transient operation, including startup. Experimental analysis of the transient performance at differently operating conditions is carried out in the present study. Table 1 lists the design specification of a LHP that is used in the present study.

The design of a LHP for the present experiment is shown in Fig. 2. A heating block was attached to the bottom of the evaporator to provide the heat load for test. The power input of the heating block was controlled by an AC power supply. Two DC fans were used to cool the condenser plate in the experiment.

Six T-type thermocouples with uncertainty of ±0.5 °C were used to measure the temperatures. The thermocouples were connected to data logger (YOKOGAWA MV200) that transfers the data to a computer through ethernet at a rate of one recording every 1 s. Another recorder WM-01 was used to measure the heating power every 1 s.

2. Derivation of system dynamics model of a LHP

From system control theory, the voltage of DC fan and the heat load are the controllable inputs. The system outputs are the temperature of the heating block (T_b) and the temperature of the compensation chamber (T_{cc}). A LHP is thus a multiple-input–multiple-output (MIMO) system, as shown in the block diagram of Fig. 3. Since a LHP is a nonlinear system, we derive the linearly perturbed model as an approximation, using perturbed variables from a steady state, e.g. $\tilde{G}_{LHP}(s)$.

The four transfer functions of a LHP model can be identified separately by isolation method. For example, $\tilde{G}_{11}(s)$ is identified with a

* Corresponding author. Tel.: +886 2 23634790; fax: +886 2 23640549.
E-mail address: bjhuang@seed.net.tw (B.J. Huang).

1359-4311/$ - see front matter © 2009 Elsevier Ltd. All rights reserved.
doi:10.1016/j.applthermaleng.2009.03.015

Nomenclature

dP/dT	the slope of the pressure–temperature, Pa/°C
G	Laplace transfer function
K	gain
M_o	the maximum overshoot, $M_o = e^{-\pi\xi/\sqrt{1-\xi^2}}$
P	pole
$\dot{Q}$	heat transfer rate, W
$\dot{Q}_{in}$	head load applied to heating block, W
RSS	root sum square
V_{fan}	voltage of fan, V
T	temperature, °C
s	complex variable in Laplace transform
t	time, s
ΔP_{tot}	total pressure drop in a LHP, Pa
ΔP_w	pressure drop in wick, Pa
Z	zero

Greek

ω_n	natural frequency, rad/s
ξ	damping ratio

Subscripts

a	ambient
b	heating block
cc	compensation chamber
cal	calculated
$crit$	critical heat load
e	evaporator
LHP	loop heat pipe
$meas$	measured
min	minimal heat load
s	overshoot of heat load

Over line

$\sim$	perturbation

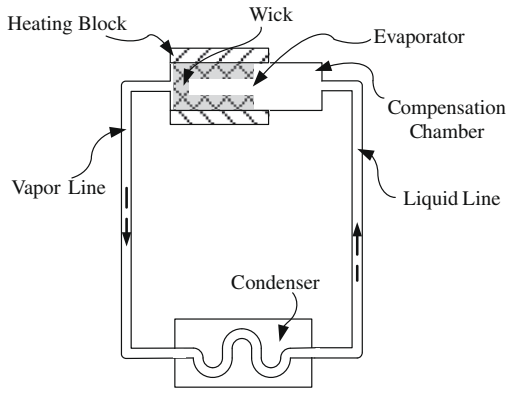

Fig. 1. Schematic of a LHP.

Table 1
Specification of a LHP used in the present study.

Evaporator	Material	Nickel powder
	Capillary force	5 cm Hg
	Porosity	60%
	Pore size	5–10 μm
	Outer diameter	14 mm
	Total length	90 mm
Connecting tube	Material	Copper (C12200)
	Outer diameter	4 mm
	Inner diameter	2.3 mm
Condenser plate	Material	Copper (C12200)
	Dimension	200 mm × 300 mm × 0.5 mm
	Cooling device	A fan on top of the plate, with adjustable fan speed by changing input voltage
Heating block	Material	Aluminum alloy 6063
	Dimension	45 mm × 40 mm × 20 mm
Working fluid	Acetone	

constant fan speed, i.e. $\tilde{V}_{fan} = 0$, while applying a step input of $\tilde{Q}_{in}$ and measuring the response of $\tilde{T}_b$. The operating conditions of the experiments are shown in Table 2.

The parameters changed depend on the different operating points. The frequency response of $\tilde{G}_{11}(s)$ at various operating points is presented in Fig. 4. The same method is applied to $\tilde{G}_{21}(s), \tilde{G}_{12}(s),$ and $\tilde{G}_{22}(s)$.

The identified parameters of $\tilde{G}_{11}(s), \tilde{G}_{21}(s), \tilde{G}_{12}(s)$ and $\tilde{G}_{22}(s)$ are listed in Tables 3 and 4. RSS is defined as

$$\mathrm{RSS} = \sum_{t=1}^{N} [T_{meas}(t) - T_{cal}(t)]^2 \tag{2}$$

where T_{meas} is the measured temperature and T_{cal} is the calculated temperature from the model.

Fig. 5 shows the comparison between the average model and the experimental data at the different operating points. We may use an average model to represent the dynamics models of LHP that are expressed in the following equations:

$$\tilde{G}_{11}(s) = \frac{\tilde{T}_b(s)}{\tilde{Q}_{in}(s)} = \frac{K_1(s+Z_1)}{(s+P_1)(s+P_2)} = \frac{0.00448(s+0.00151)}{(s+0.00553)(s+0.00138)} \tag{3}$$

$$\tilde{G}_{21}(s) = \frac{\tilde{T}_{cc}(s)}{\tilde{Q}_{in}(s)} = \frac{K_1(s+Z_1)}{(s+P_1)(s+P_2)} = \frac{0.00139(s+0.00097)}{(s+0.00458)(s+0.00098)} \tag{4}$$

$$\tilde{G}_{12}(s) = \frac{\tilde{T}_b(s)}{\tilde{V}_{fan}(s)} = \frac{K_2(s+Z_1)}{(s+P_1)(s+P_2)} = \frac{0.00693(s+0.00093)}{(s+0.005)(s+0.00095)} \tag{5}$$

$$\tilde{G}_{22}(s) = \frac{\tilde{T}_{cc}(s)}{\tilde{V}_{fan}(s)} = \frac{K_2(s+Z_1)}{(s+P_1)(s+P_2)} = \frac{0.01408(s+0.00157)}{(s+0.00945)(s+0.00148)} \tag{6}$$

From the identified model (Eqs. (3)–(6)), LHP is a stable second-order system with one zero that can be used to predict the system dynamic behaviour of a LHP. It can be noted that a model reduction can be applied to $\tilde{G}_{12}$ and $\tilde{G}_{21}$, since a pole and the zero are very close. However, the system dynamics model of a plant has to be consistent for all of its components according to the fundamental concept of system science. Besides, it will be easier for a control system design if the system dynamics models of all the components are of the same form.

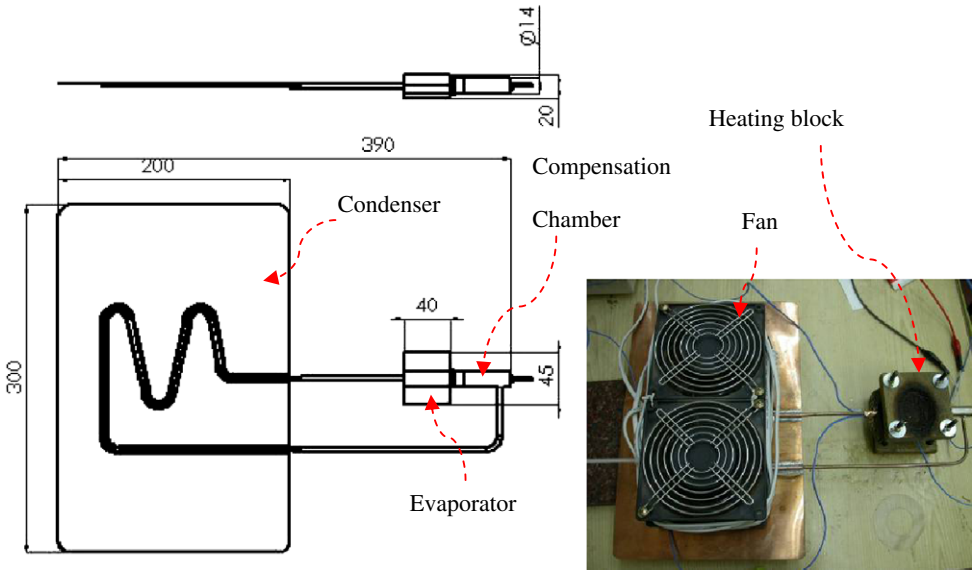

Fig. 2. Schematic of a LHP (unit: mm).

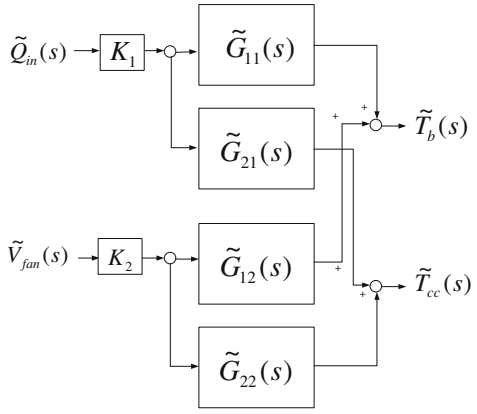

Fig. 3. The block diagram of the MIMO system.

Table 2
The operating conditions of the experiments.

Operating point	Q_{in} (W)	V_{fan} (V)
1	60 → 80	9
2	80 → 100	9
3	100 → 80	9
4	80 → 60	9
5	80	6 → 9
6	80	9 → 12
7	80	12 → 9
8	80	9 → 6

3. Startup behaviour of a LHP

The dynamic model identified above is obtained by analyzing the dynamic test data of a LHP which has been started successfully. A successful startup is defined as the case that the temperature of a LHP will reach steady state. However, the startup of a LHP may fail when the heat load is small. For a LHP used in the present study, the overshoot and the oscillation phenomena are observed at the heat load lower than 40 W. It is found that the startup phenomena of a LHP can be classified into four modes based on the heat loads:

(1) failure mode: $\dot{Q}_{in} < \dot{Q}_{min}$;
(2) oscillating mode: $\dot{Q}_{min} < \dot{Q}_{in} < \dot{Q}_{crit}$;
(3) overshoot mode: $\dot{Q}_{crit} < \dot{Q}_{in} < \dot{Q}_s$;
(4) normal mode: $\dot{Q}_s < \dot{Q}_{in}$.

The three heat loads characterizing the four modes ($\dot{Q}_{min}, \dot{Q}_{crit}, \dot{Q}_s$) can be determined experimentally.

3.1. Failure mode: $\dot{Q}_{in} < \dot{Q}_{min}$

The minimum heat load $\dot{Q}_{min}$ is defined as a condition in which a LHP can start up successfully. When the heat load is smaller than the minimum value ($\dot{Q}_{min}$), the temperature at the evaporator will continue to increase and cannot reach a steady state. The startup fails. The experimental result shows that the minimum heat load is 5 W as shown in Fig. 6.

3.2. Oscillating mode: $\dot{Q}_{min} < \dot{Q}_{in} < \dot{Q}_{crit}$

Startup experiments reveal that there is an oscillating phenomenon for $\dot{Q}_{min} < \dot{Q}_{in} < \dot{Q}_{crit}$. At this mode, the vapor flow to the condenser is not stable but in oscillating or pulsating state. The test results of Fig. 7 show that the temperature exhibits an oscillating phenomenon at $\dot{Q}_{in} = 20$ W.

In this oscillating startup mode, the temperature of the evaporator starts to increase and the vapor starts to flow into the condenser. The vapor speed response is always faster than the temperature response at the condenser. Due to the time lag of vapor condensation in the condenser, the temporary vapor accumulation in the condenser occurs and causes heat accumulation. This leads to a constant rise in the temperature of the evaporator. Once the vapor inside the condenser starts to condense, the sub-cooled liquid will start to return to the compensation chamber and the temperature of the evaporator will start to decrease. Consequently, the vapor flow rate decreases due to the decrease in the temperature of the evaporator.

In this mode, the vapor flow is high enough to push the liquid segments existing in the connecting pipes and condenser forward. Since the vapor flow is not high enough due to low heat load, once the vapor flows to some distance, vapor condensation will create a retardation force to the flow. This results in the phenomenon of

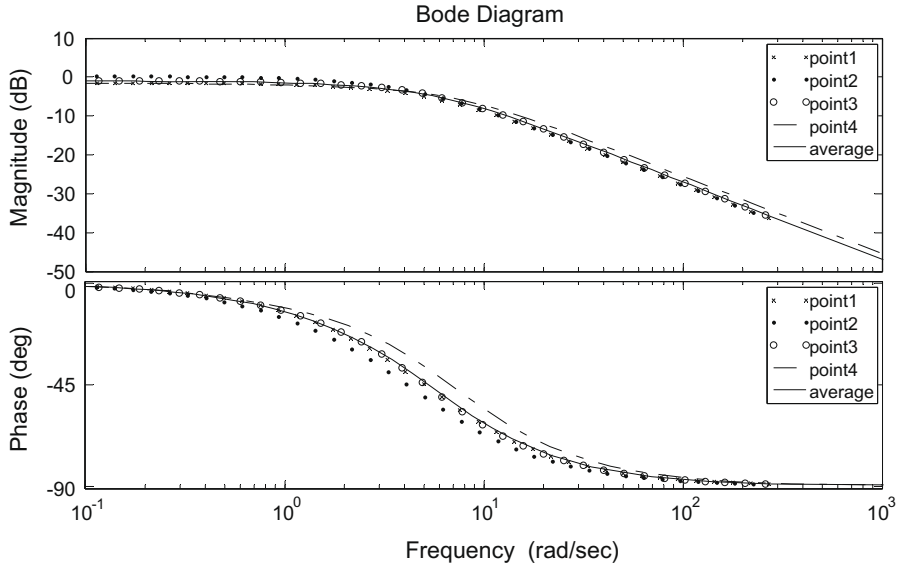

Fig. 4. Model comparison of $\tilde{G}_{11}(s)$ at the different operating points.

Table 3
The identified parameters of $\tilde{G}_{11}(s)$ and $\tilde{G}_{21}(s)$.

Model	Operating point	Heat load (W)	RSS	K_1	Z_1	P_1	P_2
$\tilde{G}_{11}(s)$	1	60 → 80	5.8712	0.0041	0.0022	0.0054	0.002
	2	80 → 100	8.3497	0.0041	0.0018	0.0045	0.0016
	3	100 → 80	7.9801	0.0044	0.0095	0.0052	0.0009
	4	80 → 60	21.5688	0.0053	0.0011	0.007	0.001
$\tilde{G}_{21}(s)$	1	60 → 80	12.7164	0.00099	0.0008	0.0032	0.0009
	2	80 → 100	8.9805	0.000962	0.0014	0.003	0.0015
	3	100 → 80	10.3471	0.0015	0.0005	0.0045	0.0005
	4	80 → 60	18.5976	0.0021	0.0012	0.0076	0.001

Table 4
The identified parameters of $\tilde{G}_{12}(s)$ and $\tilde{G}_{22}(s)$.

Model	Operating point	Voltage of fan (V)	RSS	K_2	Z_1	P_1	P_2
$\tilde{G}_{12}(s)$	5	6 → 9	12.975	0.009	0.00088	0.0048	0.0008
	6	9 → 12	5.5623	0.004	0.00085	0.0032	0.001
	7	12 → 9	3.5448	0.0065	0.0011	0.0085	0.001
	8	9 → 6	9.4071	0.0082	0.0009	0.0035	0.001
$\tilde{G}_{22}(s)$	5	6 → 9	14.9401	0.023	0.00079	0.0102	0.0008
	6	9 → 12	8.3551	0.0075	0.0016	0.0055	0.0019
	7	12 → 9	4.079	0.0092	0.001	0.0108	0.0011
	8	9 → 6	4.9071	0.0166	0.0029	0.0113	0.0021

flow oscillation or pulsation as well as temperature oscillation observed in the condenser as shown in Fig. 7. From the test results of Fig. 7, we can derive a second-order system dynamics model, Eq. (7), with oscillation period at 218 s and natural frequency 0.029 rad/s.

$$\tilde{G}(s) = \frac{\tilde{T}_b(s) - \tilde{T}_a(s)}{\tilde{Q}_{in}(s)} = \frac{\omega_n^2}{s^2 + \omega_n^2} = \frac{0.029^2}{(s + 0.029i)(s - 0.029i)} \tag{7}$$

It is shown that a LHP is an undamped system with two poles.

3.3. Overshoot mode: $\dot{Q}_{crit} < \dot{Q}_{in} < \dot{Q}_s$

As the heat load is higher than $\dot{Q}_{crit}$, a LHP enters into the overshoot mode startup and an overshoot of temperature is observed as shown in Fig. 8.

In this mode, the vapor flow is higher than the oscillation mode and is able to push the liquid segments existing in the connecting pipes and condenser forward. A retardation force to the vapor flow is, however, generated at the beginning stage by liquid segments collision and merging with vapor condensation. The vapor pressure continues to rise with the heat load and finally reaches a critical value which is able to push the liquid to return to the evaporator to complete the fluid circulation along the loop. A stable flow then starts to develop.

$$\tilde{G}(s) = \frac{(\tilde{T}_b - \tilde{T}_a)(s)}{\dot{\tilde{Q}}_{in}} = \frac{\omega_n^2}{s^2 + 2\xi\omega_n s + \omega_n^2} \tag{8}$$

According to the test results of Fig. 8, the maximum overshoot ($M_o = e^{-\pi\xi/\sqrt{1-\xi^2}}$) is 0.1127,which is the maximum peak value of the response curve, and the rise time is 139 s, which is the time

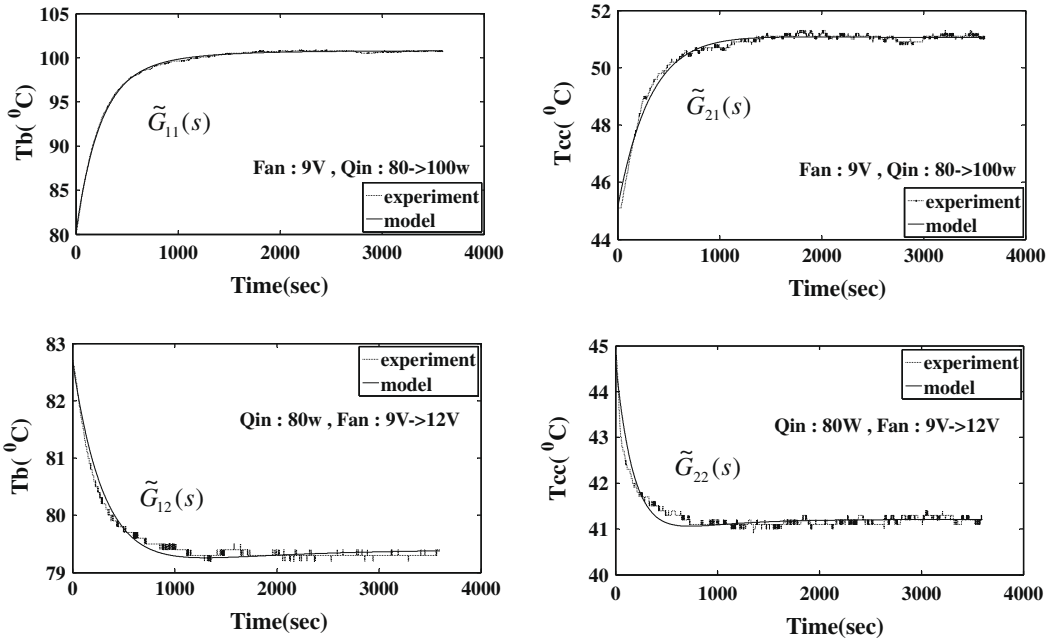

Fig. 5. Comparison of $\tilde{G}_{11}(s), \tilde{G}_{21}(s), \tilde{G}_{12}(s)$ and $\tilde{G}_{22}(s)$ between experiment and model.

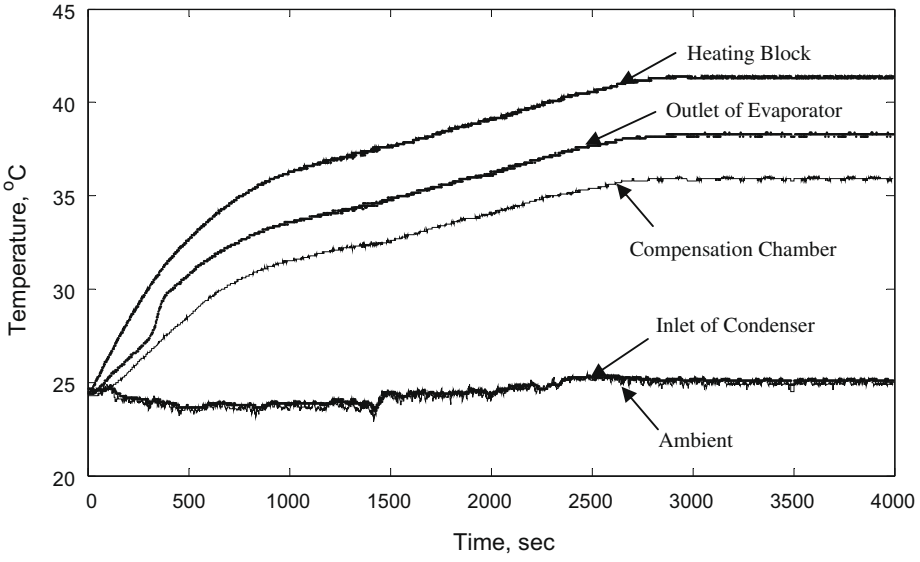

Fig. 6. Temperature response at $\dot{Q}_{in} = 5$ W.

required for a system step response to rise from 0% to 90%. The natural frequency is thus 0.013 and the damping ratio (ξ) is 0.0573 and the poles are $P = -\xi\omega_n \pm \omega_n\sqrt{1-\xi^2}i = -0.00745 \pm 0.01065i$. The system dynamics model of this mode is also of second-order which follows Eq. (8).

3.4. Normal mode: $\dot{Q}_s < \dot{Q}_{in}$

During the heat load $\dot{Q}_s < \dot{Q}_{in}$, a smooth startup is observed. Smooth transient curves which indicate a rise in the temperature of the condenser are observed. This is supposed to be the normally operated mode of a LHP which is a second-order system with one zero.

From Fig. 9, it is seen that the system dynamics model identified previously, Eqs. (3)–(6), represents the normal startup mode performance of a LHP with $\dot{Q}_s < \dot{Q}_{in}$.

4. Conclusion

This paper studies the dynamic behaviour of a LHP. The system dynamics model of a LHP is derived from the experimental results and the startup behavior is studied. It is found that the system dynamics of a LHP is a variable-structure system that changes with the operating conditions. The system dynamics in normal mode can be described by the second-order transfer functions. It is also found that the startup phenomena of a LHP can be classified into four modes, based on the heat load: (1) failure mode: $\dot{Q}_{in} < \dot{Q}_{min}$, (2) oscillating mode: $\dot{Q}_{min} < \dot{Q}_{in} < \dot{Q}_{crit}$, (3) overshoot mode: $\dot{Q}_{crit} < \dot{Q}_{in} < \dot{Q}_s$, and (4) normal mode: $\dot{Q}_s < \dot{Q}_{in}$.

The startup behaviour of a 100 W prototype in oscillating mode and overshoot mode is a second-order system. The startup behaviour of a 100 W prototype in normal mode with heat load 40–120 W is a second-order system with one zero. For heat load

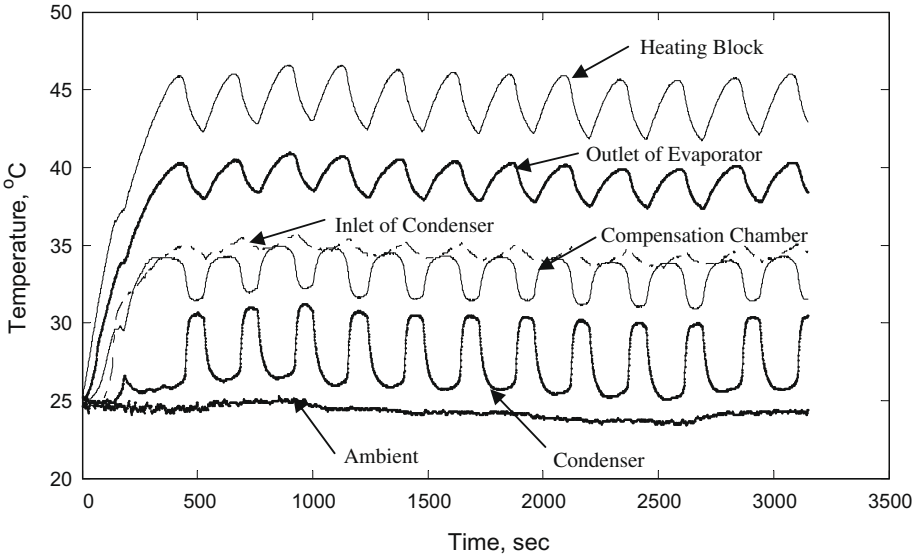

Fig. 7. Temperature response at $\dot{Q}_{in} = 20$ W.

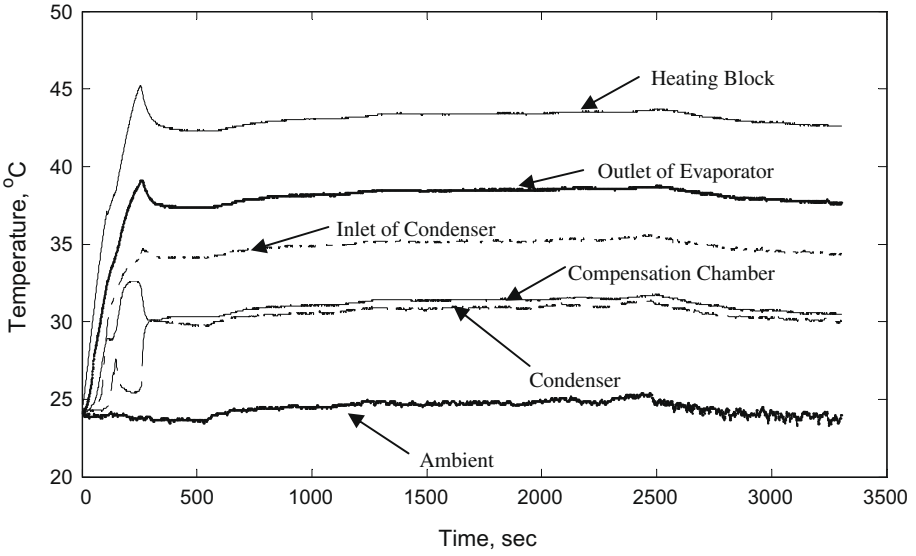

Fig. 8. Temperature response at heat load $\dot{Q}_{in} = 30$ W.

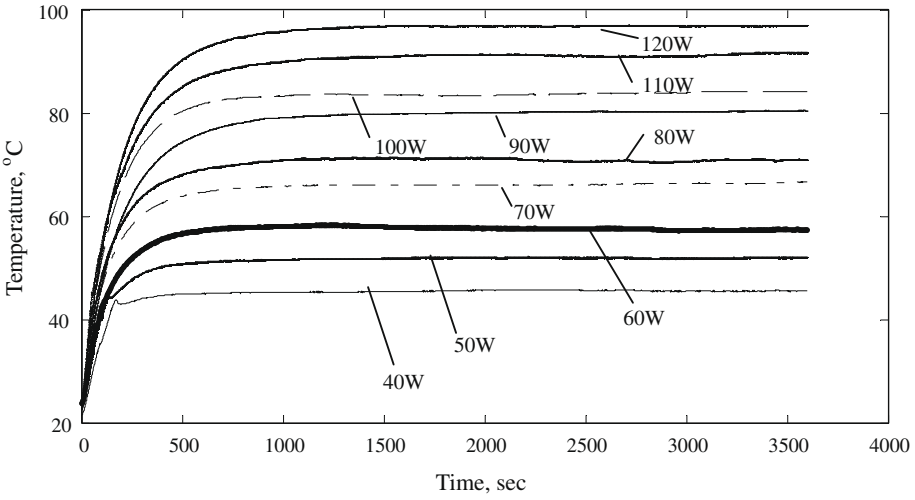

Fig. 9. Temperature response of heating block at heat load $\dot{Q}_{in}$= 40–120 W.

$\dot{Q}_{in} < 40\ \mathrm{W}(\dot{Q}_s)$, overshoot phenomenon is observed. For $20\ \mathrm{W}(\dot{Q}_{crit}) < \dot{Q}_{in} < 40\ \mathrm{W}(\dot{Q}_s)$, oscillation phenomenon is observed. For $\dot{Q}_{in} < 5\ \mathrm{W}(\dot{Q}_{min})$, the startup failure is observed.

References

[1] Yu.F. Maydanik, Review loop heat pipes, Applied Thermal Engineering 25 (2005) 635–657.

[2] R.R. Riehl, T. Dutra, Development of an experimental loop heat for application in future space missions, Applied Thermal Engineering 25 (2005) 101–112.

[3] J. Ku, Operation Characteristics of Loop Heat Pipes, SAE-Society of Automotive Engineers, Paper # 1999-01-2007, 1999.

[4] H. Nagano, J. Ku, Start-up Behavior of a Miniature Loop Heat Pipe with Multiple Evaporators and Multiple Condensers, in: 45th AIAA Aerospace Sciences Meeting and Exhibit, Reno, Nevada, 2007, AIAA 2007-1213.